Monitoring the sign reversal of the valence band exchange integral in (Ga,Mn)As

W. Heimbrodt[a,*], Th. Hartmann[a], P.J. Klar[a], M. Lampalzer[a], W. Stolz[a], K. Volz[a], A. Schaper[a], W. Treutmann[a], H.-A. Krug von Nidda[b], A. Loidl[b], T. Ruf[c], V.F. Sapega[c]

[a] *Department of Physics and Materials Science Centre, Philipps-University Marburg, Renthof 5, 35032 Marburg, Germany*
[b] *Department of Physics, University of Augsburg, Universitätsstraße 2, 86135 Augsburg, Germany*
[c] *Max-Planck-Institut für Festkörperforschung, Heisenbergstraße 1, 70569 Stuttgart, Germany*

1. Introduction

Magnetic semiconductors (MS) are promising materials for spin electronic devices, e.g. MS layers may serve as spin-filters or spin-aligners for the spin injection into non-magnetic semiconductor layers. Besides the well investigated (II,Mn)VI diluted magnetic semiconductors (DMS) with a strongly enhanced paramagnetic behaviour [1,2] (Ga,Mn)As was suggested as new material, which exhibits ferromagnetism with Curie-temperatures up to 100 K for $x_{Mn} \approx 0.05$. The advantage of (Ga,Mn)As (or even (In,Mn)As [3]) over (II,Mn)VI DMS is their

* Corresponding author. Tel.: +49-6421-2821353; fax: +49-6421-282-7036.
E-mail address: wolfram.heimbrodt@physik.uni-marburg.de (W. Heimbrodt).

compatibility with current III–V electronics and opto-electronics [4,5]. Up to now, the growth technique employed for obtaining heavily Mn-doped GaAs has been exclusively low temperature MBE. We demonstrate that (Ga,Mn)As can be successfully grown by metal-organic vapour-phase epitaxy (MOVPE), which is also of interest for industrial applications.

Currently, the sign of the p–d exchange integral $N_0\beta$ between the localised Mn moments and the extended valence band states is intensively discussed in experimental as well as theoretical work [6–11]. In the present paper, we will show that the sign of $N_0\beta$ depends on the growth conditions.

2. Experimental details

We have used *bis*-(*methylcyclopentadienyl*) *manganese* ($(MeCp)_2Mn$) as Mn-precursor, triethylgallium and tertiarbutylarsine as Ga and As sources for the MOVPE of the $Ga_{1-x}Mn_xAs$ system [6,12]. The $Ga_{1-x}Mn_xAs$ epitaxial layers were grown on (1 0 0) GaAs substrates with a thin undoped GaAs buffer in a horizontal reactor system at substrate temperatures in the range of 400°C to 550°C. The growth rate was about 1 μm/h. The epitaxial layers have been characterised by X-ray diffraction and transmission electron microscopy (TEM). Both techniques reveal the high structural quality of the $Ga_{1-x}Mn_xAs$. The magnetic and magneto-optical properties have been investigated by superconducting quantum interference device (SQUID) measurements, electron spin resonance (ESR) measurements, magneto-optical photoluminescence (PL) and PL excitation (PLE) measurements in external fields up to 7.5 T as well as spin-flip Raman spectroscopy (SFRS) in magnetic fields up to 14 T.

3. Results and discussion

Depending on the growth conditions the samples exhibit either paramagnetic or ferromagnetic behaviour. In Fig. 1a the PL of a ferromagnetic (Ga,Mn)As layer is compared to that of a paramagnetic (Ga,Mn)As layer. The peaks at about 1.514 eV are due to donor-bound excitons (D^0X) and the peaks

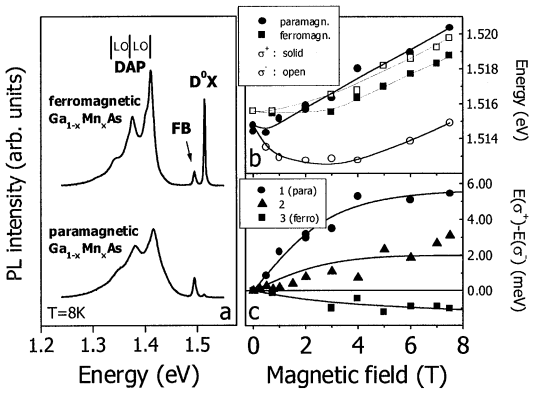

Fig. 1. (a) Photoluminescence spectra of a ferromagnetic and paramagnetic epitaxial layer. (b) Corresponding hh-exciton Zeeman-splitting as a function of magnetic field B determined by PLE. (c) Energy splitting versus B for different samples. $T = 2$ K.

at 1.495 eV are the well known carbon (C_{As}) free to bound (FB) transition [13]. These excitonic emission bands are partly buffer related. The broad emission bands (DAP) around 1.41 eV and the corresponding LO-phonon replica consisting of two series of lines originate from the (Ga,Mn)As layer. The high-energy series is the free electron to acceptor transition, whereas the weaker low-energy series must be ascribed to a donor–acceptor pair transition. The high intensity of the bands prove that Mn is incorporated as acceptor on cation sites.

The paramagnetic and the ferromagnetic samples exhibit a strong s, p–d exchange interaction between the localised magnetic moments of the Mn^{2+} ions and the extended band states, which leads to the so-called 'giant' Zeeman-splitting at low temperatures. For the heavy hole (hh) excitons the splitting can be calculated in mean field approximation:

$$\Delta E_{\mathrm{exc}} = g_{\mathrm{exc}}\mu_{\mathrm{B}}B + x_{\mathrm{Mn}} \cdot N_0(\alpha - \beta)SB_{\mathrm{S}}(\varsigma), \quad (1)$$

where $N_0\alpha$ and $N_0\beta$ are the exchange integrals of the conduction band (CB) and valence band (VB); $S = 5/2$; $B_S(\varsigma)$ is the modified Brillouin function with $\varsigma = Sg_{\mathrm{Mn}}\mu_{\mathrm{B}}B/k(T + \Theta)$; g_{exc} is the excitonic g-factor, μ_{B} is Bohr's magneton, B is the external field; $g_{\mathrm{Mn}} \approx 2$ and Θ is the Curie–Weiss parameter. Combining the results of exciton Zeeman-spectroscopy and SFRS the exchange integrals for the CB and VB can be determined separately. SFRS is sensitive to the exchange

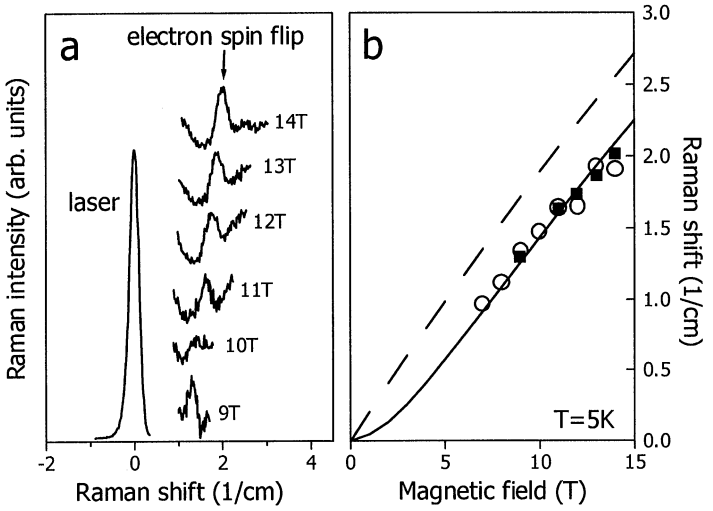

Fig. 2. (a) Spin-flip Raman scattering spectra of the conduction band electrons for various magnetic fields B. (b) Energy position of the spin-flip signal versus B.

integral of the CB only. The CB splitting is given by:

$$\Delta E_{\mathrm{CB}} = g_{\mathrm{e}}\mu_{\mathrm{B}}B + x_{\mathrm{Mn}} \cdot N_0\alpha S B_{\mathrm{S}}(\varsigma), \qquad (2)$$

where g_{e} is now the electron g-factor. In Fig. 2a typical electron SFRS spectra are depicted. The corresponding Raman-shifts are given in Fig. 2b for a paramagnetic and a ferromagnetic sample at various B-strengths. Using the $g_{\mathrm{e}} = -0.44$ for the GaAs electron [14] and its B-dependence caused by the non-parabolicity of the CB: $g^*(B) = g_{\mathrm{e}} + g_{\mathrm{B}}B$ with $g_{\mathrm{B}} = 0.0035\ \mathrm{T}^{-1}$ [15] (dashed line in Fig. 2b), it becomes evident, that $N_0\alpha$ is positive in both samples.

The hh-exciton splittings have been measured by PLE in Faraday configuration detection on the DAP and are depicted in Fig. 1bfor the paramagnetic and ferromagnetic samples as a function of B. It can be seen, that the effective excitonic coupling to the band states is ferromagnetic ($\sigma^- < \sigma^+$) in the case of the paramagnetic sample, but is antiferromagnetic ($\sigma^+ < \sigma^-$) in the case of the ferromagnetic sample. These results have been confirmed by studying various other samples by PLE and by reflection measurements. The excitonic splitting caused by the ferromagnetic coupling in the paramagnetic samples is opposite to that of undoped GaAs [6,7] and also opposite to that of all (II,Mn)VI DMS [1,2]. Since the sign of $N_0\alpha$ is unchanged (Fig. 2b), it follows, that it is actually the VB exchange integral that changes its sign with increasing Mn-content and leads to an effective antiferromagnetic coupling of the excitons in the ferromagnetic samples. It is worth mentioning, that there was some confusion and debate in recent papers about the sign of $N_0\beta$. From magnetic circular dichroism measurements it was concluded that the p–d exchange integral of (Ga,Mn)As is antiferromagnetic ($N_0\beta < 0$) [8], whereas Szczytko et al. [9] and the present authors in an earlier paper [6] reported a positive $N_0\beta$. Only recently an explanation of the ferromagnetic-type splitting was given on the basis of an antiferromagnetic p–d exchange interaction, taking into account the Moss–Burstein effect, resulting from high hole concentrations [9,10]. However, the hole concentration in our paramagnetic sample, determined by Hall-measurements, is about $10^{19}\ \mathrm{cm}^{-3}$ at 300 K and less than $10^{16}\ \mathrm{cm}^{-3}$ below 100 K. Thus, the Fermi energy at 2 K is definitely above the VB edge. Therefore the considerations in Refs. [9 and 10] do not apply to our sample and we state, that in the paramagnetic case $N_0\beta$ is positive.

In Fig. 1c the Zeeman-splitting for three samples is depicted after subtracting the normal Zeeman contribution ($g_{\mathrm{exc}}\mu_{\mathrm{B}}B$). The exciton g-value ($g_{\mathrm{exc}} = 0.84$) has been determined from the hh-Zeeman splitting of

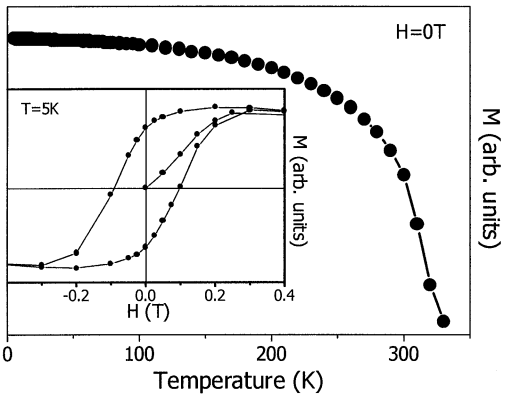

Fig. 3. Temperature dependence of the remanence of a ferromagnetic (Ga,Mn)As epitaxial layer. Inset: corresponding hysteresis at $T = 5$ K.

an undoped GaAs-epilayer [6]. Again the opposite signs of the exchange integrals for the paramagnetic sample (curve 1) and for the ferromagnetic sample (curve 3) are obvious. Curve 2 has been measured on a sample with somewhat higher Mn-concentration than the paramagnetic sample. From Eq. (1) one would therefore expect a larger excitonic splitting. However, the measured splitting is considerably smaller. Even for that sample we can exclude from our Hall-measurements a Moss–Burstein effect. In what follows, we show that the sign reversal mechanism is correlated with the occurrence of ferromagnetism.

Fig. 3 depicts a typical hysteresis at 5 K and the remanence curve as a function of temperature of a ferromagnetic (Ga,Mn)As-epilayer with high Mn concentration measured by SQUID. It is worth pointing out, that the Curie temperature is above 300 K, which is essential for applying this material in spin electronics. The reason for the room temperature ferromagnetism is the formation of microclusters of Mn(Ga)As within the paramagnetic (Ga,Mn)As host (see Fig. 4). The cluster size detected by bright-field TEM investigations is about 80–100 nm in diameter and about 150–200 nm in height. No dislocations are observable in the entire layer structure. Specific microscopic investigations are in progress to clarify the structure, crystalline orientation and chemical composition of the clusters [16]. The formation of MnAs clusters has been reported by various authors for as-grown high-temperature MBE samples [17] as well

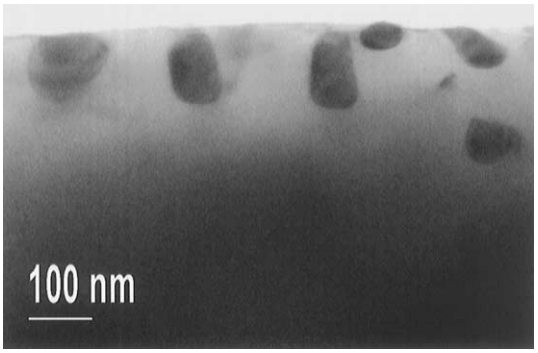

Fig. 4. Bright field TEM micrograph of a Mn(Ga)As clusters within the paramagnetic (Ga,Mn)As host.

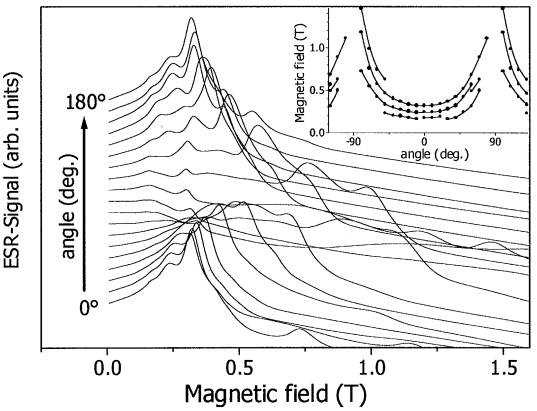

Fig. 5. ESR spectra of the ferromagnetic sample in dependence on the angle between sample normal and magnetic field (0° to 180°). $T = 50$ K. Inset: Positions of the main peaks versus the angle between the sample normal and magnetic field (−120° to 120°).

as low-temperature MBE samples after post-growth annealing [18,19].

Fig. 5 depicts typical ESR spectra measured on a ferromagnetic sample using an X-band spectrometer. Details will be discussed elsewhere. These signals are not observable in our paramagnetic samples. A distinct feature of the ESR spectra is a strong anisotropy detectable when changing the angle between the sample normal and *B*-axis. The inset shows the 180° symmetry of the anisotropy, which is caused most likely by the easy axis of the sample magnetisation. It is interesting to note, that we were also able to detect a weak ESR signal of this kind for sample 2 of Fig. 1c, although, for this sample, the ferromagnetism was not

detectable by SQUID and no large clusters were detected by TEM. We conclude, that this sample is at the threshold of micro-cluster formation.

Correlating the information about the ferromagnetism with the magneto-optical results allows one to tentatively determine absolute values for the exchange integrals in the paramagnetic and ferromagnetic case. The concentration-independent ratio $R = N_0\alpha/[N_0(\alpha - \beta)]$ can be determined very accurately for each sample using Eqs. (1) and (2) in the saturation range of the Brillouin-function, whereas for a determination of absolute values of the exchange integrals a very precise knowledge of the Mn concentration x_{Mn} is needed. For the paramagnetic sample used in Fig. 1 x_{Mn} was determined by SIMS measurements to be about 0.001 in agreement with Hall-data. In the case of the ferromagnetic sample, actual and effective Mn concentration need to be distinguished. As we discuss the exchange splitting of the band states of the (Ga,Mn)As host material and not the bandstructure of the ferromagnetic clusters, the effective x_{Mn} is that within the host material and is of comparable magnitude to that of the paramagnetic sample. In what follows, we assume that the effective x_{Mn} are 0.001 for the paramagnetic and the ferromagnetic sample. The best fit for the paramagnetic sample in Fig. 1c yields $x_{Mn}N_0(\alpha-\beta)=-2.5$ meV, whereas the respective fit in Fig. 2 gives $x_{Mn}N_0\alpha=2.3\cdot10^{-2}$ meV. Thus, we derive:

$$\frac{N_0\alpha}{N_0\beta} = \frac{R}{R-1} \cong 0.01. \qquad (3)$$

This is a surprisingly small ratio for the absolute values of the exchange integrals. In the case of the (II,Mn)VI DMS the absolute value of the VB exchange integral $N_0\beta$ is known to be only about 4–5 times larger than $N_0\alpha$. We tentatively deduce $N_0\beta = +2.5$ eV and $N_0\alpha=+0.023$ eV in the paramagnetic case. For the ferromagnetic sample, we obtain from Fig. 2b the same $x_{Mn}N_0\alpha$ as in the paramagnetic case, but a different $x_{Mn}N_0(\alpha - \beta)$ from Fig. 1c. Using the experimental ratio $N_0\alpha/N_0\beta = -0.083$ yields $N_0\beta = -0.28$ eV in the ferromagnetic case. Obviously, two different p–d coupling mechanisms must be present in the paramagnetic and ferromagnetic regimes. Therefore, the absolute values of $N_0\beta$ can be considered only as lower limits of the 'pure' exchange integrals, i.e. both values might be partly compensated by the competing mechanism. The smaller exciton splitting of the sample 2 in Fig. 1c may be the result of a beginning compensation mechanism of the VB exchange integrals caused by the occurrence of microscopic ferromagnetic clusters. There is no or a much weaker compensation of the CB exchange integral.

4. Conclusions

MOVPE growth of high quality (Ga,Mn)As layers is possible. Excitonic transitions are observable even at higher x_{Mn}. The reversal of sign of the VB exchange integral $N_0\beta$ is monitored. At very low x_{Mn}, we find a ferromagnetic p–d coupling which becomes partly compensated by an antiferromagnetic coupling with increasing x_{Mn}. This compensation is related to the formation of ferromagnetic Mn(Ga)As clusters.

Acknowledgements

Funding by the DFG (SFB 383 and the Graduate College "Optoelectronics of Mesoscopic Semiconductors") is gratefully acknowledged.

References

[1] J.K. Furdyna, J. Appl. Phys. 64 (1988) R29.
[2] O. Goede, W. Heimbrodt, Phys. Stat. Sol. B 146 (1988) 11.
[3] H. Munekata, H. Ohno, S. von Molnar, A. Segmüller, L.L. Chang, L. Esaki, Phys. Rev. Lett. 17 (1989) 1849.
[4] H. Ohno, Science 281 (1998) 951.
[5] A. Van Esch, L. Van Bockstal, J. De Boeck, G. Verbanck, A.S. van Steenbergen, P.J. Wellmann, B. Grietens, R. Bogaerts, F. Herlach, G. Borghs, Phys. Rev. B 56 (1997) 13103.
[6] Th. Hartmann, M. Lampalzer, W. Stolz, K. Megges, J. Lorberth, P.J. Klar, W. Heimbrodt, Thin Solid Films 364 (2000) 209.
[7] J. Szczytko, W. Mac, A. Stachow, A. Twardowski, P. Becla, J. Tworzydlo, Solid State Commun. 99 (1996) 927.
[8] K. Ando, T. Hayashi, M. Tanaka, A. Twardowski, J. Appl. Phys. 83 (1998) 6548.
[9] J. Szczytko, W. Mac, A. Twardowski, F. Matsukura, H. Ohno, Phys. Rev. B 59 (1999) 12935.
[10] A. Twardowski, Mat. Sci. and Eng. B 63 (1999) 96.
[11] A.K. Bhattacharjee, C. Benoit a la Guillaume, Solid State Commun. 113 (2000) 17.
[12] M. Lampalzer, W. Treutmann, J. Pebler, K. Megges, J. Lorberth, W. Stolz, P.J. Klar, W. Heimbrodt, K. Volz, A. Schaper, in preparation.

[13] B. Hamilton, Semiconductors Semimetals 38 (1993) 286.
[14] M. Oestreich, W.W. Rühle, Phys. Rev. Lett. 74 (1995) 2315.
[15] V.F. Sapega, T. Ruf, M. Cardona, Solid State Commun. 114 (2000) 573.
[16] K. Volz, M. Lampalzer, A. Schaper, J. Zweck, W. Stolz, P.J. Klar, W. Heimbrodt, in preparation.
[17] H. Akinaga, S. Miyanishi, K. Tanaka, W. Van Roy, K. Onodera, Appl. Phys. Lett. 76 (2000) 97.
[18] J. Wellmann, J.M. Garcia, J.-L. Feng, P.M. Petroff, Appl. Phys. Lett. 71 (1997) 2532.
[19] J. De Boeck, R. Oesterholt, A. Van Esch, H. Bender, C. Bruynseraede, C. Van Hoof, G. Borghs, Appl. Phys. Lett. 68 (1996) 2744.